



HAL
open science

Secondary Injectant Gas Thermodynamic Properties Effects on Fluidic Thrust Vectoring Performances of a Supersonic Nozzle

A. Chpoun, M. Sellam, V. Zmijanovic, L. Léger

► **To cite this version:**

A. Chpoun, M. Sellam, V. Zmijanovic, L. Léger. Secondary Injectant Gas Thermodynamic Properties Effects on Fluidic Thrust Vectoring Performances of a Supersonic Nozzle. 30th International Symposium on Shock Waves, 1, Springer; Springer International Publishing, pp.539-543, 2017, 10.1007/978-3-319-46213-4_92 . hal-02398154

HAL Id: hal-02398154

<https://univ-evry.hal.science/hal-02398154v1>

Submitted on 4 Jun 2021

HAL is a multi-disciplinary open access archive for the deposit and dissemination of scientific research documents, whether they are published or not. The documents may come from teaching and research institutions in France or abroad, or from public or private research centers.

L'archive ouverte pluridisciplinaire **HAL**, est destinée au dépôt et à la diffusion de documents scientifiques de niveau recherche, publiés ou non, émanant des établissements d'enseignement et de recherche français ou étrangers, des laboratoires publics ou privés.



Distributed under a Creative Commons Attribution 4.0 International License

Secondary Injectant Gas Thermodynamic Properties Effects on Fluidic Thrust Vectoring Performances of a Supersonic Nozzle

A. Chpoun, M. Sellam, V. Zmijanovic, and L. Leger

Introduction

The transverse injection in a supersonic cross-flow is problematic which can be encountered in several aerodynamic applications such as fuel injection in scramjet combustor, missile control, drag reduction, and thrust vector control. In recent years, an extended analytical, numerical, and experimental work has been carried out by the authors [1, 2] to investigate the vectoring performances of a supersonic axisymmetric nozzle using secondary fluid injection. Secondary gas injection thrust vector control (SITVC) or shock vector control (SVC) is considered as an alternative way to control the thrust direction of a rocket nozzle beside the classical use of mechanical device such as fluidic actuators. In the context of SITVC operation, the nature and source of injectant gas may raise efficiency-related issues. In previous studies [3–6], it is well established that injection of gas with low molar mass promotes better jet penetration and therefore will be a better choice for SITVC operation. To assess this point, an experimental test campaign has been conducted in the hypersonic test facility EDITH of the CNRS institute ICARE in Orléans, France. The focus of the study is to analyze the secondary injectant gas thermodynamic properties influence on the global vectoring performance of a supersonic nozzle. For this purpose, performance aspects of fluidic thrust vectoring concept have been experimentally investigated on a truncated ideal contour (TIC) nozzle model using a variety of gas species (with low to moderate molar mass) as injectant. Qualitative and quantitative diagnostics consisted of Z-Schlieren

visualization, 3-axis force balance, and static and dynamic parietal pressure measurements. The experimental results are compared to the numerical and analytical findings.

Analytical and Numerical Approaches

The cross injection of a secondary sonic jet into a main supersonic flow due to its practical relevance was extensively investigated by many authors. In some works, the phenomenon was analytically modeled [7]. The main purpose of the analytical model was to draw a relation between the injectant fluid properties, the main and secondary flows stagnation conditions, and the secondary jet penetration height as a main relevant parameter. In short, the analytical model was based on the concept of the secondary flow acting as a blunt body vis-à-vis the main flow (Fig. 1). The 1D momentum and mass conservation laws are applied to the flow surrounding the obstacle. Depending on the geometry of the injection orifice, circular or slot, the fluidic obstacle is assumed as being a quarter sphere or a quarter cylinder, respectively. The model necessitates additional correlations for the magnitude of the plateau pressure and the flow separation region beginning and extension. Later, the analytical approach was successfully applied by Mangin [7] to the shock-induced thrust vector control of a planar (2D) nozzle. The present analytical model proposed by the authors is an extension to axisymmetrical nozzle of the latest mentioned work. It fully takes into account the axisymmetrical nature of the flow for the pressure gradient and the boundary layer calculations. A detailed description of the model can be found in Ref. [2].

For the numerical part of the work, a finite-volume 3D code CPS developed by Bertin and CNES (Centre National d'Etudes Spatiales) for propulsive nozzle flows has been employed. The code solves Favre Averaged Navier–Stokes (FANS) equations for compressible multispecies reacting flows with fully accounted viscous effects on an unstructured 3D computational grid. Time splitting is used for the

A. Chpoun (✉) • M. Sellam
Laboratoire de Mécanique et d'Énergétique d'Evry LMEE, Université
d'Evry Val d'Essonne, 40 rue du Pelvoux, 91020 Evry Cedex, France
e-mail: a.chpoun@iut.univ-evry.fr

V. Zmijanovic • L. Leger
Institut ICARE/CNRS, 1C avenue de la recherche scientifique,
Orléans, France

explicit scheme of order up to four in time and up to three in space. The fluxes are computed on the cell interfaces with HLLC (by Toro) scheme or Roe's upwind difference splitting scheme for ideal gases. In the present study, flux vectors are evaluated at each time step using a second-order scheme. The turbulence is modeled using the classical $k - \epsilon$ closure. Main airflow and secondary gas injectant are modeled as perfect gases with power-law expressions for $\gamma(T)$ and $C_p(T)$ as seventh degree polynomials. Integration is achieved with a fully explicit solver, setting the time step control range from unsteady for highest time accuracy to the steady optimized time step with the Courant–Friedrichs–Lewy (CFL) condition parameter up to 0.3.

Figure 2 shows a typical mesh used in the computations. It contains 5.15 million mapped hexagonal elements in the nozzle domain and 1.05 million in the exterior domain. Preliminary studies of grid convergence have been carried out. The final computations were done and are presented here according to the conclusions drawn from the preliminary studies.

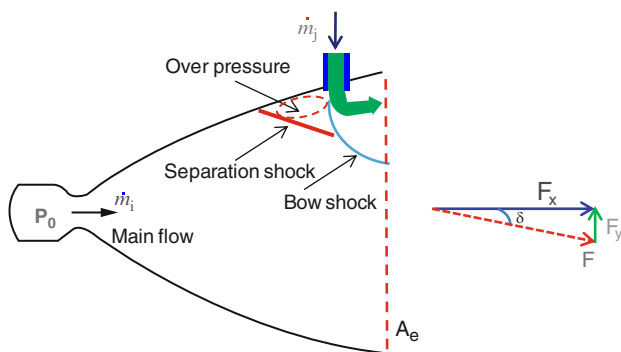
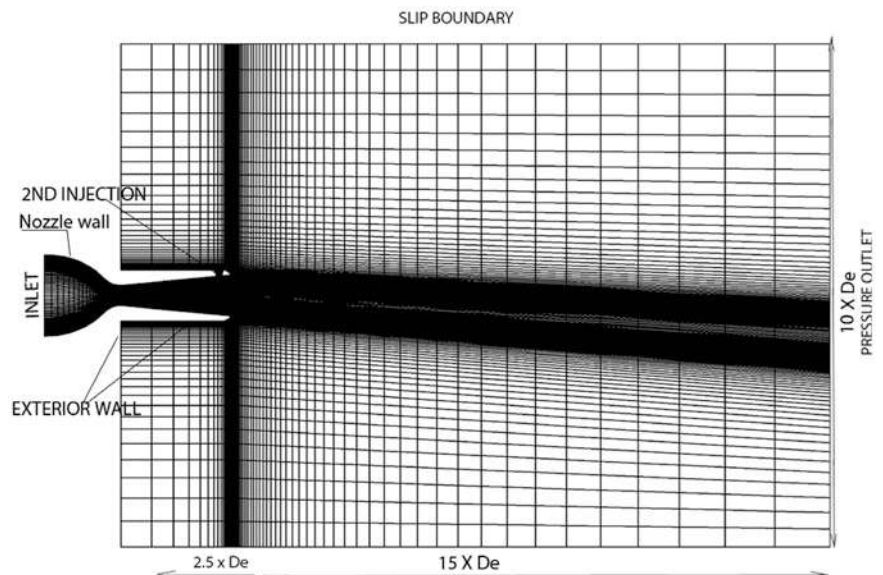


Fig. 1 Schematic view of fluidic thrust vectoring

Fig. 2 A typical mesh used in computations



Experimental Work

The experiments were conducted in the EDITH hypersonic/supersonic test facility of ICARE/CNRS institute at Orléans, France. Initially, it was a continuous running Mach 5 wind tunnel supplied with 9 bars total pressure by a volumetric compressor. At downstream side, the pressure in the test chamber is lowered by two powerful volumetric vacuum pumps of a total 345 KW power. The authors modified the installation in order to perform tests on small-scale nozzle. Small test nozzles were placed inside the test chamber to take advantage of high vacuum environment supplied by pumps. It permits to simulate high-altitude operation conditions. In the modified version of the installation, clean, oil-free air is first dried, compressed till 300 bars, and stored in several 320 L tanks. The air is supplied via 8 mm pipeline system to a pressure regulator and after to a radial flow splitter. Through six uniformly distributed 8 mm tubes, air is supplied to the settling chamber of 160 mm diameter and 200 mm length and exhausted through the nozzle into the depressurized tunnel test section.

The secondary flow gas is furnished to a second settling chamber and then smoothly injected via a convergent duct into the tested nozzle. For the secondary flow, pressurized 80 L bottles are used as the source for helium, argon, carbon dioxide, and nitrogen tests. A schematic view of the test bench is given in Fig. 3.

Results

The investigation was conducted to examine four injectant gas species of different molar mass (air, He, CO₂, Ar) (Table 1) on two major injection condition sets: setting the

Fig. 3 Experimental installation

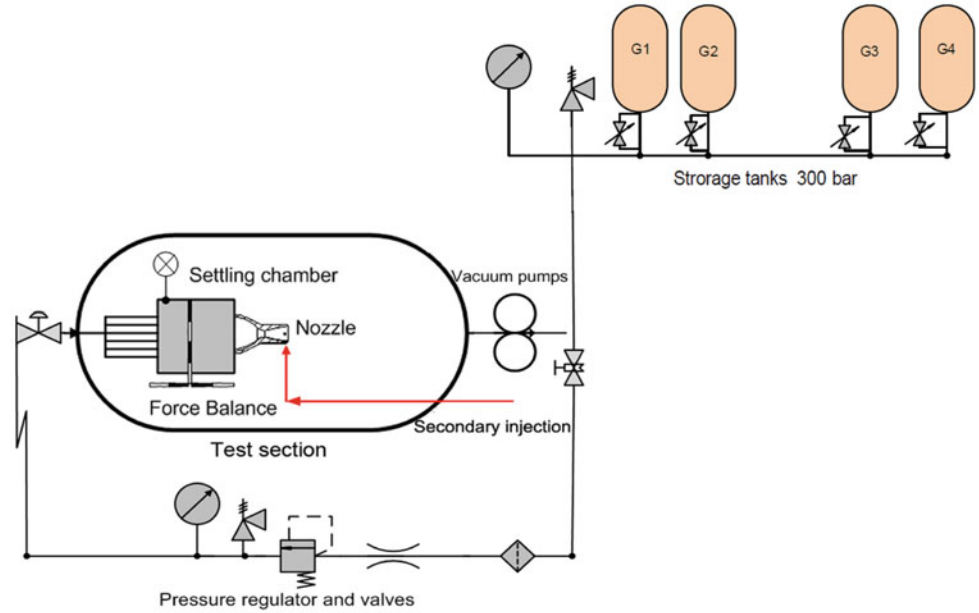


Table 1 Thermodynamic gas properties and corresponding injection conditions

	M_{gj}	γ_{gj}	$M_{gj}\gamma_{gj}$	f_m (SPR = 1)	SPR (P_{0j}/P_0) ($f_m = 0.076$)
Air	28.960	1.4	40.544	0.076	1.
He	4.0026	1.66	6.6698	0.03	2.534
Ar	39.948	1.66	66.460	0.095	0.803
CO ₂	44.009	1.29	57.080	0.091	0.833

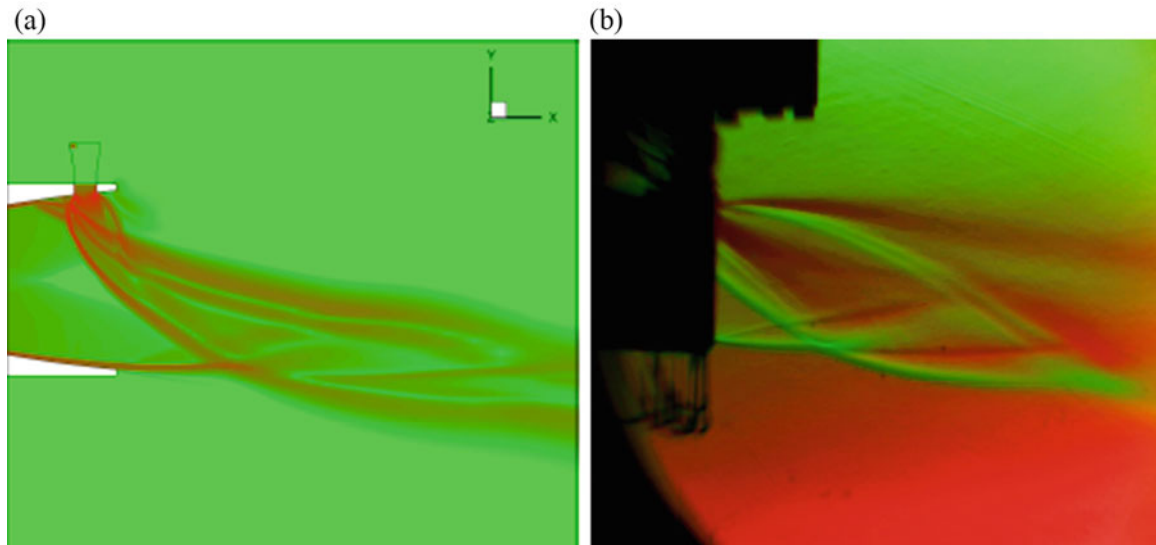


Fig. 4 Numerical (a) and experimental (b) Schlieren for SPR = 1 (CO₂ into Air)

constant secondary injection pressure ratio (SPR) for all species and by setting constant the secondary to the main flow mass flow rates f_m .

Figure 4 shows the flow topology extracted from numerical results (left) by plotting density gradients and that

obtained by bicolor Schlieren technique. The case corresponds to the injection of a secondary flow of carbon dioxide into the main airflow for SPR = 1. The two visualizations show a global di-symmetry in flow topology resulting in side forces. The flow structures are similar from

both approaches. The difference between the two pictures can be explained by the difference between the two visualization techniques; the numerical Schlieren represents the extracted density gradient on the plane of symmetry, whereas the experimental Schlieren technique integrates these density gradients over the full depth of the nozzle jet flow. It is worth to mention that the flow details inside the nozzle can only be shown from numerical results. However, both pictures show the fluidic obstacle bow shock leaving the nozzle and interacting with the expanding jet boundary.

Iso-Mach contours in the symmetry plane of the nozzle from numerical simulations are presented in Figure 5. The left (a) and middle (b) plots correspond, respectively, to the injection of argon and carbon dioxide which have close molar mass, whereas the right (c) plot corresponds to the injection of helium with a lower molar mass. In all cases, the secondary mass flow rates were the same corresponding to a secondary to the main flow mass flow rates of $f_m = 0.076$. Numerical results show that in the case of helium injection, the secondary jet penetrates deeper inside the nozzle resulting in a more extended flow separation zone. Therefore, the performance

of helium-based SITVC operation is better than those employing argon and carbon dioxide.

Tables 2 and 3 show, respectively, the vectoring performances in term of thrust deviation angle δ for different injectant/main flow gas couples and for different secondary injection conditions. From these results, it is evident that it is possible to achieve better vectoring performance for the same pressure ratio with smaller mass flow rate as is the case of a lighter gas as helium comparing to the more inert gas species. In other words, one can achieve a far better deviation angle with the same mass flow rate using helium as injectant.

As a consequence, the mass of injectant gas required for a launcher controlling task can be divided by a factor of two or more depending on the molar mass of the gas.

This trend is also depicted in Fig. 6 which shows comparison between numerical, analytical, and experimental approaches for the thrust vectoring angle evolution versus the ratio of injectant to the main flow gas product of gas molar mass and specific heats ratio. It is well known that this parameter plays a dominant role in the jet penetration phenomenon. The comparison between numerical, analytical,

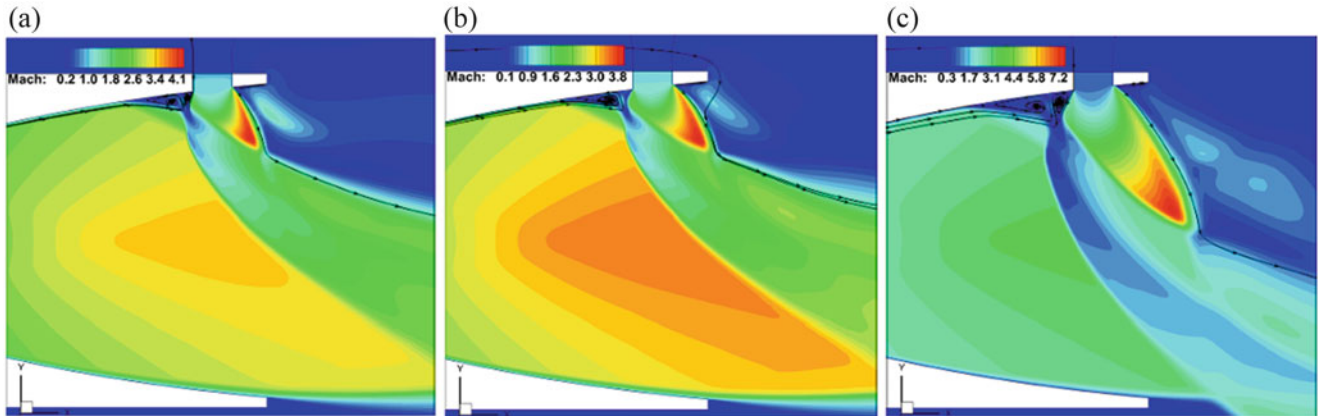


Fig. 5 Mach contours plots, (a) Ar-Air, (b) CO₂-Air, (c) He-Air, in symmetry plane of the TIC nozzle at $f_m = 0.076$

Table 2 Force components and thrust vector pitch angle at SPR = 1

	f_m	$\Sigma F_{y num}[N]$	$\Sigma F_{y exp}[N]$	$\Sigma F_{y mod}[N]$	$\Sigma F_{x num}[N]$	$\Sigma F_{x exp}[N]$	$\Sigma F_{x mod}[N]$	$\delta [^\circ]_{num}$	$\delta [^\circ]_{exp}$	$\delta [^\circ]_{mod}$
Air-air	0.076	16.473	16.37	16.03	136.21	131.1	134,23	6.89	7.1 ± 0.5	6.81
He-air	0.0303	16.958	18.6	16.27	136.13	133.1	134,23	7.10	8.0 ± 0.5	6.91
Ar-air	0.096	16.615	17.13	17,27	136.22	130.8	134,23	6.95	7.4 ± 0.5	6.91
CO ₂ -air	0.092	16.135	16.55	15.93	136.97	130.2	134,23	6.76	7.2 ± 0.5	6.76

Table 3 Force components and thrust vector pitch angle at $f_m = 0.076$

	SPR	$\Sigma F_{y num}[N]$	$\Sigma F_{y exp}[N]$	$\Sigma F_{y mod}[N]$	$\Sigma F_{x num}[N]$	$\Sigma F_{x exp}[N]$	$\Sigma F_{x mod}[N]$	$\delta [^\circ]_{num}$	$\delta [^\circ]_{exp}$	$\delta [^\circ]_{mod}$
Air-air	1.0	16.473	16.37	16.03	136.21	131.1	134,23	6.89	7.1	6.81
He-air	2.534	39.251	/	34.18	135.11	/	134,53	16.20	/	14.25
Ar-air	0.803	13.967	12.7	14.06	135.94	129.6	134.16	5.87	5.6	5.98
CO ₂ -air	0.833	13.062	10.42	13.46	135.68	139.8	134.16	5.49	4.6	5.73

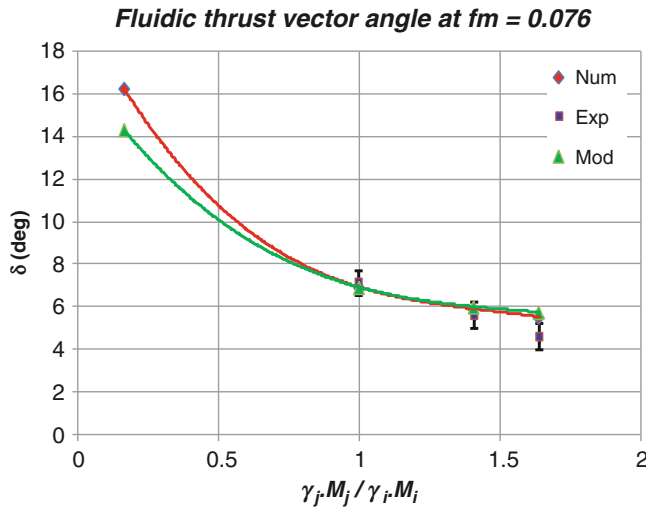


Fig. 6 Fluidic thrust vectoring angles

and experimental methods shows the same trend and gives close results considering error margin in all these triple approaches.

Summary and Conclusion

Supersonic nozzle thrust vector control by mean of secondary fluid injection has been investigated experimentally, numerically, and analytically. The main focus of the study was to investigate the injectant gas thermodynamic properties on vectoring efficiency. The study showed that significant vectoring angle (up to 15°) can be achieved with secondary to primary mass flow rates ratio of 7.5 %. Employing lower molar mass gas such as helium can lead to a vectoring efficiency of approximately $2^\circ/\%$ (degree per percent of secondary to primary flow mass flow rates). Whereas this efficiency is close to $1^\circ/\%$ for usual gas (air into air) injection. For fixed injection conditions, it was found that vectoring angle is higher when the injected gas $M_j \gamma_j$ product is less than $M_i \gamma_i$ of the primary gas. Moreover,

the experimental results, confirmed by the numerical calculations and by those from the analytical model, showed that the injection of a gas such as helium can produce the same deflection with a much lower injection mass flow rate.

Finally, as it is found that the secondary total pressure and the sonic velocity of the species are dominant over the injected mass flow rate, a scaling law relation can be given between the reciprocal specific heat ratio and molecular mass product and the performance coefficients. Smaller $M_j \gamma_j$ largely ameliorates the performance curves, while the heavy and small specific heat ratio gases are on the lower performance end.

Acknowledgment This work was supported by French space agency CNES, acknowledgments and gratitude to the S. Palerm and J. Oswald for supporting and helping us on this project. Our thanks also go to N. Gouillon and E. Depussay for their technical assistance during the experiments.

References

1. Zmijanovic, V., Lago, V., Sellam, M., Chpoun, A.: Thrust shock vector control of an axisymmetric conical nozzle via transverse gas injection. *Shock Waves J.* **24**, 97–111 (2014)
2. Sellam, M., Chpoun, A., Zmijanovic, V., Lago, V.: Fluidic thrust vectoring of an axisymmetrical nozzle: An analytical model. *Int J Aerodyn.* **2**, 193–209 (2012)
3. Wing D.J., Giuliano V.J.: Fluidic thrust vectoring of an axisymmetric exhaust nozzle at static conditions. *ASME FEDSM.* 97–3228 (1997).
4. Waithe K.A., Deere K.A.: Experimental and computational investigation of multiple injection ports in a Convergent-Divergent nozzle for Fluidic Thrust Vectoring. *AIAA paper 2003–380*. 21st AIAA Applied Aerodynamics Conference, Orlando, Florida, (2003)
5. Spaid, F.W., Zukoski, E.E.: Study of the interaction of gaseous jets from transverse slots with supersonic external flows. *AIAA. J.* **6**(2), 205–212 (1968)
6. Zukoski, E.E.: Turbulent boundary-layer separation in front of a forward-facing step. *AIAA. J.* **5**(10), 1746–1753 (1967)
7. Mangin B., Chpoun A., Jacquin L.: Experimental and numerical study of the fluidic thrust vectoring of a two-dimensional supersonic nozzle. *AIAA paper 2006–366*. 24th AIAA Applied Aerodynamics Conference San Francisco, California, (2006)